

Partitioning of Non-ionic Surfactants Between CO₂ and Brine

Albert Barrabino^{1,†}, Torleif Holt¹, Erik Lindeberg²

¹Petroleum Department, SINTEF Industry, NO-7465 Trondheim, Norway.

²CO₂ Technology, NO-7030 Trondheim, Norway.

[†]Correspondence: albert.barrabino@sintef.no

Abstract: The partitioning of non-ionic surfactants in a CO₂/synthetic brine system was studied for a selection of surfactants at reservoir conditions for CO₂ enhanced oil recovery and aquifer storage. Alkyl and alkylphenol ethoxylates with different degrees of branching in their hydrophobic moiety were chosen. Generally, higher temperature and pressure promoted increased solubility in CO₂. Branching of the hydrophobic moiety tends to favour CO₂ solubility (higher partition coefficient). Highly branched moieties were found to hinder solubility probably due to a decrease of their conformational entropy. The addition of an aromatic ring connecting the ethoxylate moiety and the hydrophobic moiety seemed to have an adverse effect at lower temperatures. For two surfactants, the effect of concentration on partitioning was also studied. The partition coefficient decreased for increasing concentrations until a plateau was reached above the corresponding surfactant critical micelle concentration (CMC). This may indicate micelle formation both in the CO₂ and in the aqueous phase.

Keywords: Mobility control of CO₂, foam, enhanced oil recovery, aquifer storage, surfactant partitioning

1. Introduction

CO₂ is becoming a prominent solvent for different applications. Its foams and emulsions with water are of interest due to its potential for various applications (Johnston and Rocha, 2009). Two large scale applications are enhanced oil recovery (EOR) and subsurface sequestration. However, these methods encounter various technical challenges. The relatively low density and low viscosity of CO₂ can lead to gravity segregation and viscous fingering giving early CO₂ breakthrough and poor volumetric sweep efficiency. The result of this may be low oil recovery (in EOR) and reduced utilisation of the storage capacity (in CO₂ sequestration) (Solbakken *et al.*, 2013; Tsau and Grigg, 1997).

Early breakthrough can be counteracted by decreasing the mobility of the CO₂. This can be achieved by increasing the viscosity using additives to the CO₂ or by dispersing the CO₂ into another fluid (brine). It is not easy to increase CO₂ viscosity. The additives (direct thickeners) must solubilize in CO₂ and provide self-interactions that can give the desired viscosity enhancement. During decades efforts have been made trying to find suitable additives (Enick *et al.*, 2012). However, the best CO₂ additives found are not practical due to their high costs and detrimental environmental impact.

The second method for decreasing CO₂ mobility is through creating dispersed systems. CO₂-in-brine dispersions (hereafter called foams) may have high apparent viscosities depending on the surfactant used. Foams can also be formed and stabilized by nanoparticles. Even though nanoparticles adsorb more strongly at interfaces, larger energy input is required to form foam. This criterion is not met at reservoir flow velocities which typically do not exceed few feet/day (except close to injection wells) (Binks, 2002; Espinosa *et al.*, 2010; San *et al.*, 2016; Yu *et al.*, 2012).

Surfactant-stabilized foam is so far the most promising CO₂ mobility reduction method. However, this also faces several challenges. One potential problem is the presence of oil which may destabilize foam through different mechanisms including spreading and entering phenomena (Manlowe and Radke, 1990; Schramm and Novosad, 1990; Wasan *et al.*, 1994). However, the sensitivity of foam to oil may have

45 both advantageous and disadvantageous consequences. During miscible CO₂ flooding, the foam may be
46 more stable in pores where the oil has already been displaced helping to divert CO₂ within the reservoir
47 to places where the oil is not displaced. There, the lamella will collapse and release CO₂ in the CO₂/oil
48 front. On the other hand, if the stability of the foam is sensitive to minute oil residues it can have an
49 adverse impact on foam propagation (Vassenden *et al.*, 2000).

50 Another challenge to face during surfactant-stabilized foam flooding is surfactant depletion due to
51 adsorption on the pore walls of the reservoir rock. The adsorption will be determined by the pore wall
52 mineralogy and charge, type of surfactant, pH, temperature, ionic strength, electrolyte concentration
53 (Bera *et al.*, 2013; Curbelo *et al.*, 2007). In traditional foam technology, the surfactant is transported in
54 the denser water phase. At some distance from the injection well, the surfactant solution and CO₂ will
55 segregate and foam cannot be formed. If the surfactant is transported in the CO₂, foam may be formed
56 wherever gas and water coexist.

57 Mobility control can also be beneficial for aquifer storage of CO₂. In order to increase the storage
58 capacity and to avoid excessive build-up of pressure, formation water must be produced from the
59 formation. The total storage capacity of a formation can be significantly increased if the volumetric
60 sweep is improved. This can reduce the total storage cost if low-cost CO₂ soluble surfactants giving
61 suitable mobility control at low flow rates can be identified (Grimstad *et al.*, 2018).

62 Efforts for finding and developing CO₂ soluble surfactants have been made since early 1990. The first
63 effective surfactant developed was fluorinated (Hoeftling *et al.*, 1991). These types of surfactants are
64 impractical due to their environmental impact and high costs. Since then, the effort has been focused on
65 finding non-fluorinated surfactants. Due to the amphiphilic nature of surfactants, CO₂-soluble
66 surfactants will also dissolve in the aqueous phase and thus, partition between both phases. CO₂
67 solubility and partitioning has been studied for several surfactant types such as dioctyl sodium
68 sulfosuccinates (AOT) (Le *et al.*, 2008), linear and branched alkylphenol ethoxylates (McLendon *et al.*,
69 2012; Xing *et al.*, 2010), branched alkyl ethoxylates (Xing *et al.*, 2012), ethoxylated cocoamines (Chen
70 *et al.*, 2012) and triblock copolymer surfactants (Adkins *et al.*, 2010).

71 However, the partition and solubility studies reported in the literature only give values for specific
72 temperatures, pressures and surfactant concentrations, and it is difficult to find data on how the
73 partitioning is influenced by changes in these variables for CO₂-brine systems.

74 Injection of surfactant through the CO₂ phase was introduced by Le *et al.* with promising core flooding
75 results. With this novel injection strategy, the surfactant dissolved in the CO₂ phase will partition to the
76 formation brine and foam can be formed in-situ, obtaining a delayed CO₂ breakthrough and an increased
77 oil recovery (Le *et al.*, 2008).

78 Knowing how partitioning is affected by pressure and temperature is important for foam flooding since
79 the mobility and strength of the foam depends on the surfactant concentration, which depends on
80 surfactant adsorption onto rock and partitioning between the phases (Ashoori *et al.*, 2009). Partitioning
81 of surfactant and its concentration dependence are therefore important input data for a foam simulator.

82 The objective of the current work was to determine the CO₂ partition coefficients in CO₂-brine systems
83 for a selection of commercially available non-ionic surfactants at variable pressures and temperatures
84 relevant for CO₂ enhanced oil recovery and CO₂ aquifer storage on the Norwegian Continental Shelf.
85 The dependence of CO₂ partitioning with varying surfactant concentration was also addressed.

86 **2. Materials and Methods**

87 **2.1. Gas**

88 The CO₂ was obtained by AGA A.S. (99.7 %).

89 **2.2. Synthetic seawater**

90 The synthetic seawater (SSW) composition used in this study is shown in Table 1. The SSW was filtered
91 through 0.45 μm cellulose nitrate filters.

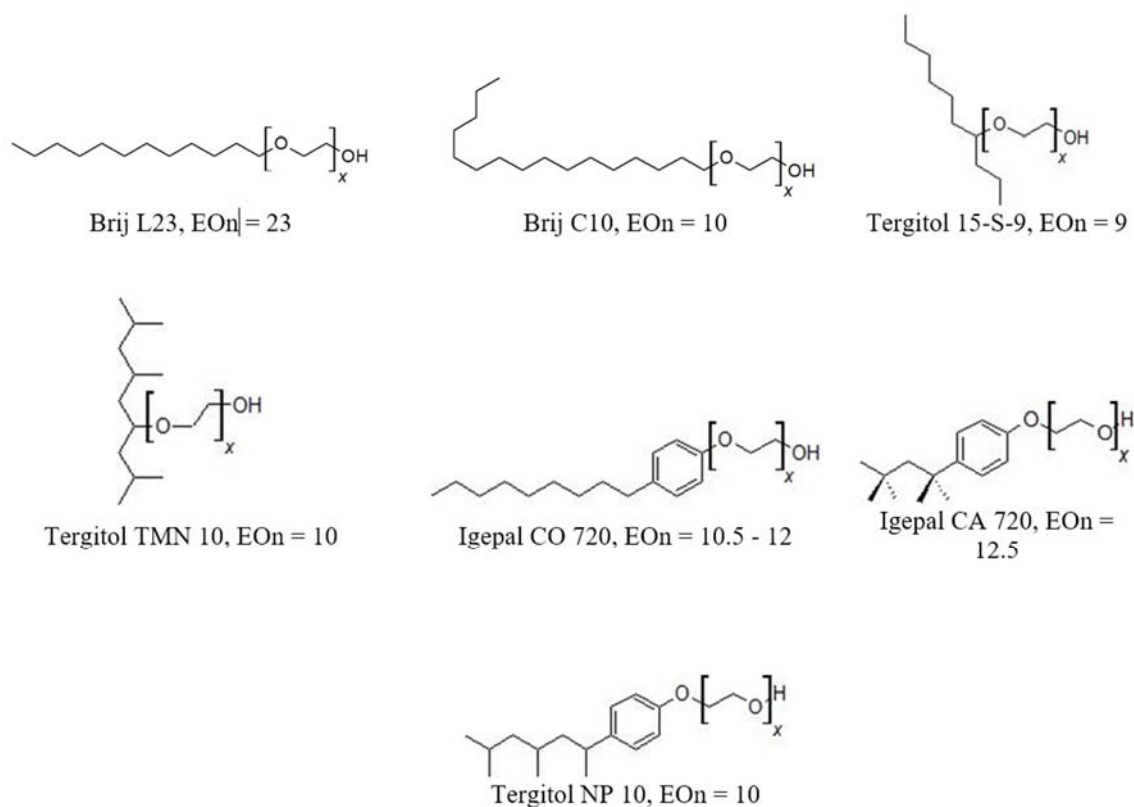
92 **Table 1.** Synthetic seawater composition.

Salt	Conc. [g/l]
NaCl	23.612
CaCl ₂ ·2H ₂ O	1.911
MgCl ₂ ·6H ₂ O	9.149
KCl	0.746
Na ₂ SO ₄	3.407

93

94 **2.3. Surfactants**

95 A selection of non-ionic surfactants was chosen for the CO₂ partitioning studies. The surfactants were
96 divided into two groups, alkyl ethoxylates and alkylphenol ethoxylates. Each group had hydrophobic
97 tails ranging from linear to highly branched alkyl groups. The surfactant chemical structures used are
98 described in Figure 1.



99

100 **Figure 1.** Surfactant chemical structures (EOn symbolizes the average number of ethoxy groups).

101 All surfactants were obtained from Sigma-Aldrich with a concentration of 100 wt.% of active material
102 except for Tergitol TMN 10, which was obtained with a concentration of 90 wt. % of active material.

103 3. Experimental

104 3.1. Cloud point determination

105 0.5 wt.% surfactant in SSW was placed in a water bath equipped with a temperature controller. The
106 temperature of the water bath was slowly increased using small increments until the cloud point of each
107 solution was observed.

108 3.2. Measurement of surfactant partitioning

109 Measurements of surfactant partitioning were performed in a high-pressure high-temperature pVT-cell
110 with an internal piston for pressure/volume control (DB Robinson). The cell temperature was controlled
111 by a heating cabinet with circulating air. A volume of 15 ml of aqueous surfactant solution was injected
112 into the cell kept at the desired temperature for the measurement. Afterwards, the cell was filled with
113 45 ml of CO₂ and the pressure was adjusted to the desired value. Once the cell was filled, the pressure
114 was kept constant by using a computer-controlled pump connected to the hydraulic side of the cell. The
115 cell was tilted 50° - 60° to increase the contact area between the phases. Then the system was left under
116 static conditions for 24 h.

117 After 24 h, a sample of approximately 6 - 8 ml of aqueous phase was extracted at a low rate, keeping
118 constant pressure inside the cell by moving the cell piston (assisted by the computer-controlled system).
119 Before collecting the sample, approximately 2 ml of sample were discarded. During the extraction
120 process, the system in the cell never exceeded 2 bar deviation from the target pressure. The extracted
121 sample was collected for further analysis.

122 3.3. Surfactant Analysis

123 The surfactant concentration in SSW was determined by HPLC using a LC-4A HPLC from Shimadzu.
124 The oven (Shimadzu CTO-2AS) was set at 50°C. The column used was a Supelcosil LC-18 (250 mm –
125 4.6 mm, 5 μm) and the samples were injected through a Rheodyne 7125 injector with a 20 μl loop. A
126 refractive index detector from Showa Denko K.K (RI SE-51) was used to detect the peaks. The
127 chromatograms were processed with the PowerChrom 180R system from eDAQ.

128 The eluent was prepared from measured amounts of methanol (HPLC grade from VWR) and water
129 (obtained from a purification system PURELAB-Option Q DV-25). The methanol:water volume ratio
130 used was 85:15 and the eluent had a concentration of 0.2 M NaNO₃ (analysis grade from Merck). The
131 eluent was filtrated through a 0.45 μm nylon membrane and continuously degassed with helium.

132 3.4. Determination of partition coefficient

133 The partition coefficient, k_p , is determined by the expression in Eq. 1.

$$134 \quad k_p = \frac{\frac{m_{sCO_2}}{m_{sCO_2} + m_{CO_2}}}{\frac{m_{sw}}{m_{sw} + m_w}} \quad (1)$$

135 where, m_{sCO_2} is the mass of surfactant dissolved in CO₂, m_{CO_2} the mass of CO₂, m_{sw} the mass of
136 surfactant dissolved in the aqueous phase, and m_w the mass of aqueous phase. The solubility of water
137 in CO₂ and CO₂ in water were neglected.

138 Some initial tests were done with surfactant dissolved in distilled water (0.5 wt.%) and CO₂. The total
139 volume was 60 ml (15 ml aqueous phase, 45 ml of CO₂) and the experiments were carried at room
140 temperature and 100 bar. In these tests, the aqueous samples were obtained as detailed above.
141 Afterwards, a large and known volume of CO₂ was extracted from the cell and flashed to ambient
142 pressure at a very low rate. The cell pressure was constant at 100 bar. The CO₂ extracted from the cell
143 was passed through a water trap. After the flash, the flow line from the cell to the trap was washed with

144 water. With known total masses of water and extracted CO₂ HPLC analysis of the water enabled the
 145 determination of m_{sCO_2} . Then, m_{sCO_2} determined by HPLC was compared to m_{sCO_2} determined by mass
 146 balance based on m_{sw} (Table 2).

147 **Table 2.** Surfactant masses and partition coefficients determined by analysing both phases (HPLC) and only aqueous phase
 148 (M.B.) for pure water/CO₂ systems at room temperature and 100 bar.

Surfactant	M.B. m_{sCO_2} [g]	HPLC m_{sCO_2} [g]	M.B. k_p	HPLC k_p
Tergitol 15-S-9 (1)	0.031	0.031	0.28	0.28
Tergitol 15-S-9 (2)	0.034	0.029	0.33	0.28
Tergitol TMN 10 (1)	0.028	0.026	0.23	0.23
Tergitol TMN 10 (2)	0.028	0.029	0.23	0.22

149

150 The two methods for determining the surfactant mass dissolved in CO₂ and the partition coefficient gave
 151 same results. Thus, it was decided to proceed by only analysing the aqueous phase and determine m_{sCO_2}
 152 from the surfactant mass balance. In this manner the measurements could be performed more rapidly.

153 In order to ensure that the systems were in equilibrium at the time of sampling, a series of sampling tests
 154 were performed to determine the equilibration time required. It was observed that 20 h were enough for
 155 the systems to have unalterable concentrations of surfactant in both phases, so it was decided that all
 156 systems would age 24 h in the cell to ensure equilibrium.

157 4. Results

158 4.1. Cloud point determination

159 The cloud points for the surfactants used are shown in Table 3. For Brij L23 was not possible to
 160 determine the cloud point due to its high value (above 100°C). The solution of 0.5 wt.% Brij C10 in
 161 SSW was already cloudy at room temperature. This was unexpected since it is specified to be above
 162 50°C (1 wt.% in water) from its producer. This surfactant was discarded for further measurements.

163 **Table 3.** Measured cloud points in SSW (0.5 wt.%).

Surfactant	Cloud Point [°C]
Tergitol 15-S-9	50
Tergitol NP 10	55
Tergitol TMN 10	70
Igepal CO 720	75
Igepal CA 720	80
Brij L23	> 92

164

165 4.2. Partition coefficients

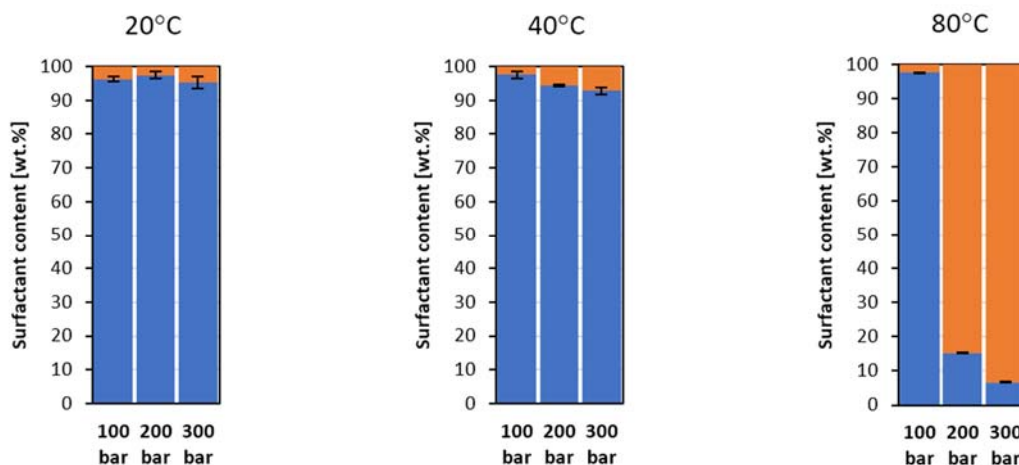
166 Determination of partition coefficients was carried out at pressures of 100, 200, and 300 bar, and at room
 167 temperature, 40°C, and 80°C. The room temperature was typically around 20 – 22°C but is hereafter
 168 referred to as 20°C. All measurements were repeated at least twice. The error bars in the figures show
 169 the standard deviation for each experimental condition.

170 4.2.1. Linear alkyl ethoxylates

171 *Brij L23*

172 Brij L23 showed low CO₂ solubility at room temperature and at 40°C. Figure 2 depicts the surfactant
 173 distribution in each phase for the studied conditions. More than the 90 wt.% of the surfactant remained
 174 in the SSW at temperatures of 20°C and 40°C. However, the surfactant content in CO₂ increased
 175 significantly at pressures of 200 and 300 bar when the temperature was increased to 80°C. It can be

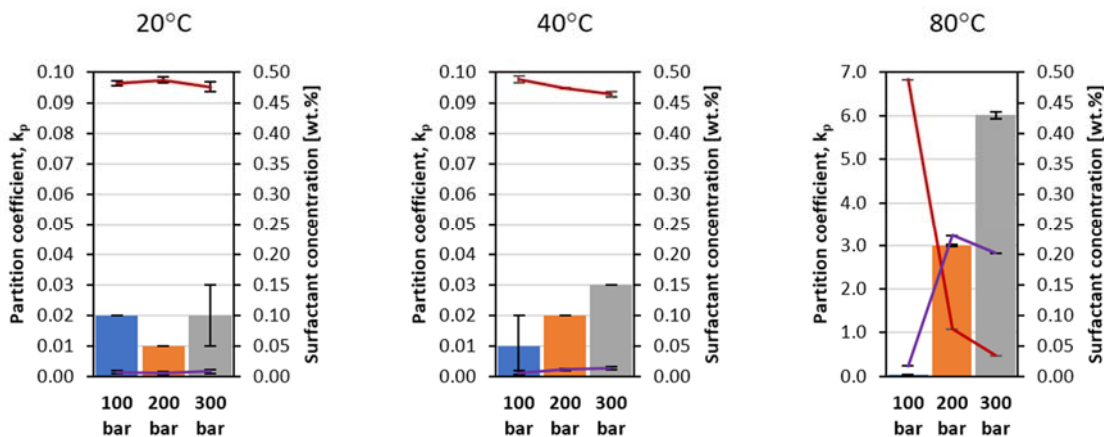
176 observed how the 85 wt.% of the surfactant migrated towards the CO₂ phase when the pressure was
 177 200 bar. At 300 bar, the 93 wt.% was found solubilized in the CO₂ phase.



178

179 **Figure 2.** Surfactant distribution in SSW (blue) and in CO₂ (orange) for Brij L23.

180 Figure 3 depicts the partition coefficients, the surfactant concentrations in SSW, and the surfactant
 181 concentration in CO₂. At room temperature, the variation of the partition coefficient with pressure was
 182 almost negligible. At 40°C, a trend to increase the partition coefficient with increasing temperature was
 183 seen. A significant pressure effect on the partition coefficient was observed at 80°C. Note that the scale
 184 of the partition coefficients varies in Figure 3 and the following figures.



185

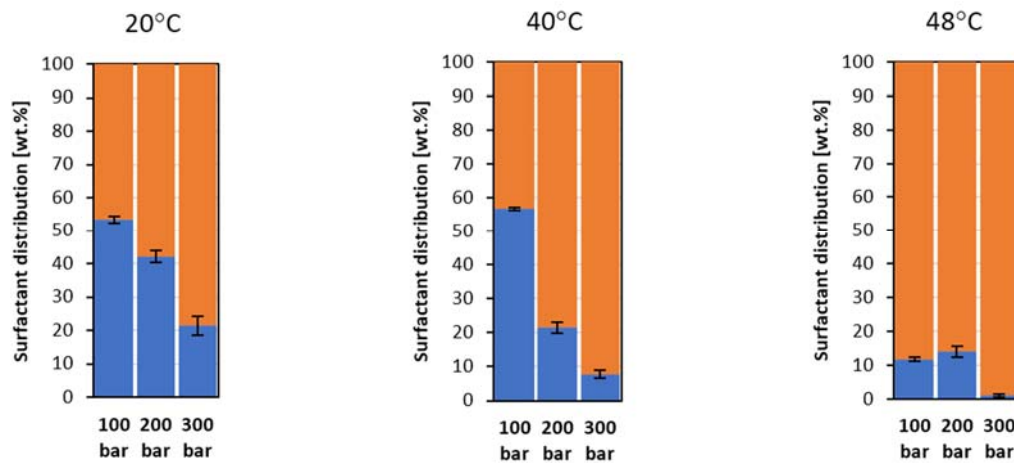
186 **Figure 3.** Partition coefficients for Brij L23 (bars). In red line, surfactant concentration in SSW; in purple, surfactant
 187 concentration in CO₂.

188 The concentration of surfactant decreased in SSW and increased in CO₂ as the partition coefficient was
 189 increased. However, at 80°C, this trend was not followed for the surfactant concentration in CO₂ for
 190 pressures of 200 and 300 bar. The decrease in concentration was due to the constant volume condition
 191 during the measurements. At 300 bar, 45 ml of CO₂ corresponds to 33.9 g CO₂ (0.746 g/ml) while, at
 192 200 bar, the mass of 45 ml CO₂ was 26.8 g (0.594 g/ml). The mass of surfactant solubilized into the CO₂
 193 was, therefore, larger at 300 bar (0.069 g) compared to 200 bar (0.062 g). The increase of the CO₂ mass
 194 when the system was at 300 bar, translates into a lower surfactant concentration.

195 4.2.2. Branched alkyl ethoxylates

196 *Tergitol 15-S-9*

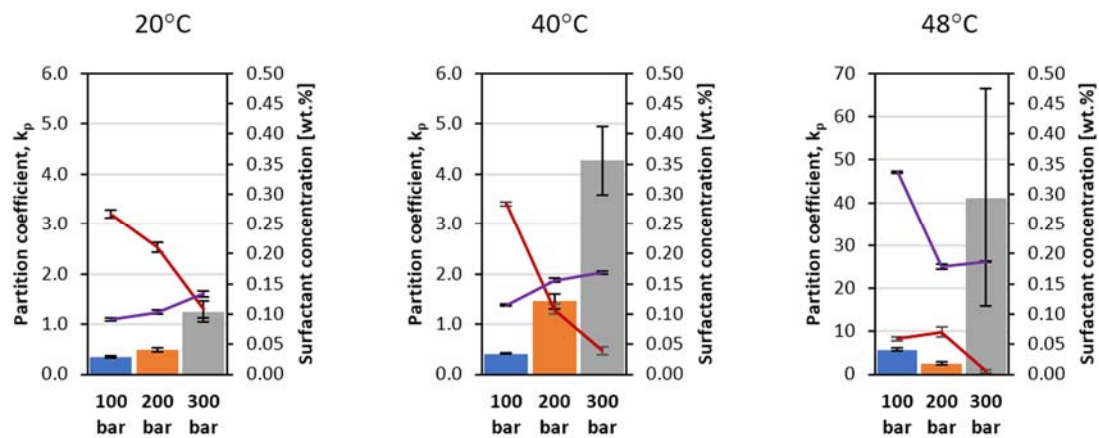
197 Of all surfactants studied in this work, Tergitol 15-S-9 showed the highest partition in CO₂ at room
 198 temperature. At 100 bar, 47 wt.% of the surfactant solubilized into the CO₂ (Figure 4). A temperature
 199 increase from 20°C to 40°C did not promote any significant variation. When the temperature was
 200 increased further approaching the cloud point (2°C below), a significant solubility increase in the CO₂
 201 phase was observed. Increased pressure increased the surfactant preference for the CO₂ phase. Both at
 202 200 bar and 300 bar the partition towards the CO₂ phase increased significantly with increased
 203 temperature. At 300 bar and 48°C, only 0.9 wt.% of the surfactant remained in SSW.



204

205 **Figure 4.** Surfactant distribution in SSW (blue) and in CO₂ (orange) for Tergitol 15-S-9.

206 The partition coefficient increased as temperature and pressure increased (Figure 5). At 48°C, no
 207 significant variation of the surfactant concentration in SSW was observed at 100 bar and 200 bar.
 208 However, a significant decrease in the surfactant concentration in the CO₂ was observed at these
 209 conditions. This decrease was partly a consequence of density effects, as explained before. As seen in
 210 Figure 4, the surfactant content in the CO₂ phase decreased from 88 wt.% (100 bar) to 86 wt.% (200 bar).
 211 Due to the mentioned effect, the decrease in the concentration was from 0.34 wt.% to 0.18 wt.%.



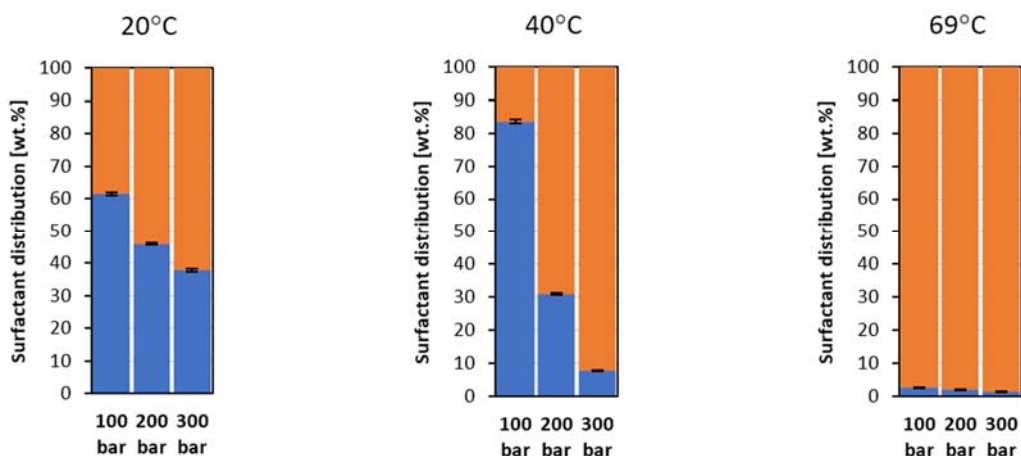
212

213 **Figure 5.** Partition coefficients for Tergitol 15-S-9 (bars). In red line, surfactant concentration in SSW; in purple, surfactant
 214 concentration in CO₂.

215

216 *Tergitol TMN 10*

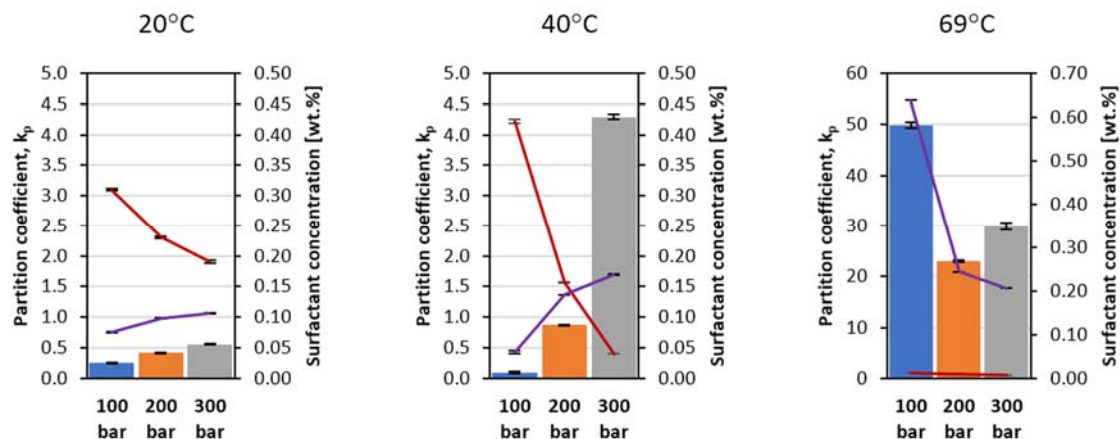
217 Tergitol TMN 10 also exhibited a preference for the CO₂ phase. The surfactant solubility in the CO₂
218 phase increased with pressure (Figure 6). Increased temperature also promoted surfactant partitioning
219 towards the CO₂ phase except at 100 bar when the temperature was increased from 20°C to 40°C where
220 the surfactant content in the CO₂ decreased from 39 wt.% to 16 wt.%. At 69°C, the residual surfactant
221 in SSW decreased to 2.6 wt.%, 2.1 wt.% and 1.3 wt.% at 100 bar, 200 bar and 300 bar, respectively.
222 Tergitol TMN 10 was highly CO₂-philic at this temperature.



223

224 **Figure 6.** Surfactant distribution in SSW (blue) and CO₂ (orange) for Tergitol TMN 10.

225 The partition coefficient increased as pressure increased for 20°C and 40°C (Figure 7). However, at 100
226 bar the partition coefficient decreased when the temperature increased from 20°C to 40°C. At 69°C, a
227 deviation from this trend was observed. The highest coefficient was obtained at 100 bar. When the
228 pressure was increased to 200 bar, the coefficient decreased significantly. A further increase of pressure
229 to 300 bar resulted in an increased partition coefficient. The surfactant concentration in the CO₂ phase
230 decreased. Meanwhile, the surfactant content in the same phase increased (Figure 7 and Figure 6). This
231 observation is explained by the density effect as explained previously.



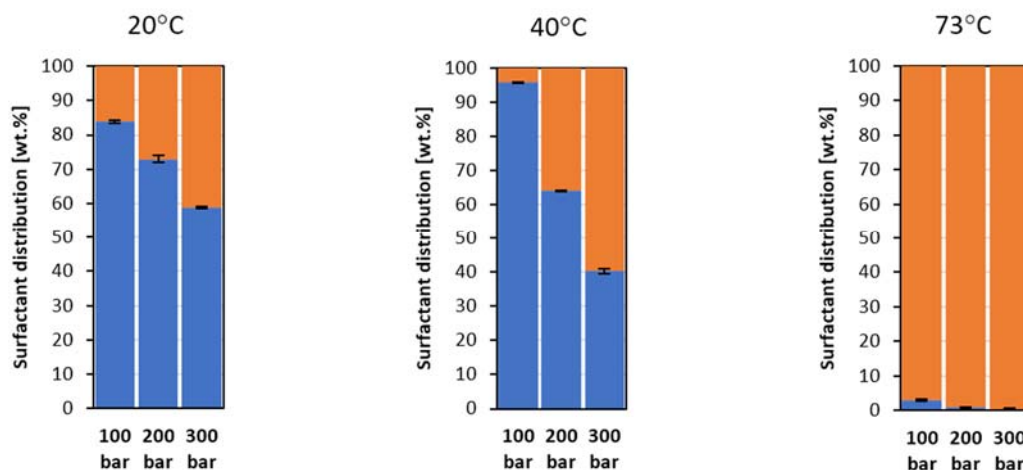
232

233 **Figure 7.** Partition coefficient for Tergitol TMN 10 (bars). In red line, residual surfactant concentration in SSW; in purple,
234 surfactant concentration in CO₂.

235 4.2.3. Linear alkylphenol ethoxylates

236 *Igepal CO 720*

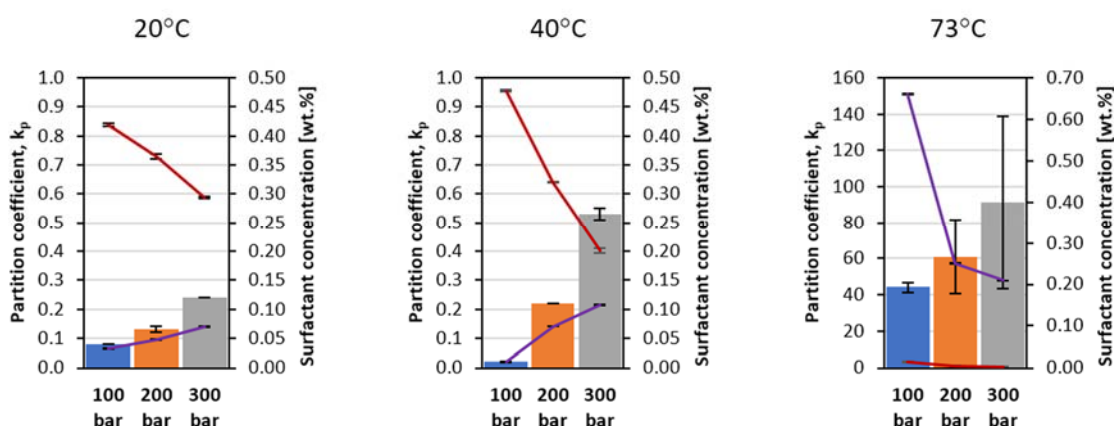
237 The preference of Igepal CO 720 for the CO₂ phase generally increased as both temperature and pressure
 238 increased (Figure 8). One exception was observed at 100 bar, however. When the temperature increased
 239 from 20°C to 40°C the surfactant content in the CO₂ phase decreased. This surfactant had preference for
 240 the CO₂ phase as the temperature approached its cloud point (75°C, see Table 3). At this temperature,
 241 the content of surfactant in SSW was 3.0 wt.%, 0.8 wt.%, and 0.4 wt.% at pressures of 100 bar, 200 bar,
 242 and 300 bar, respectively.



243

244 **Figure 8.** Surfactant distribution in SSW (blue) and in CO₂ (orange) for Igepal CO 720.

245 The partition coefficient followed the expected trend, it increased with temperature and pressure (Figure
 246 9). The same exception was observed at 100 bar at temperatures of 20°C and 40°C, where the
 247 partitioning coefficient decreased for increasing temperature.



248

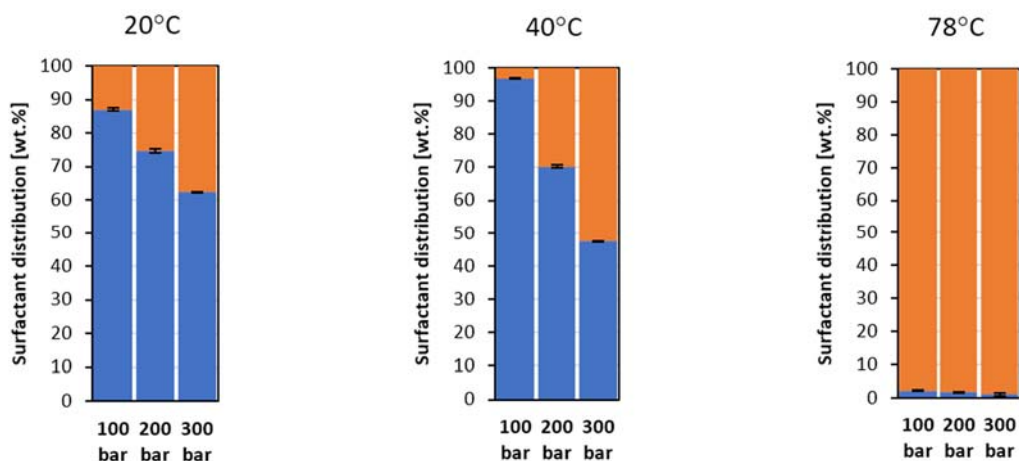
249 **Figure 9.** Partition coefficient for Igepal CO 720 (bars). In red line, residual surfactant concentration in SSW; in purple,
 250 surfactant concentration in CO₂.

251

252 4.2.4. Branched alkylphenol ethoxylates

253 *Igepal CA 720*

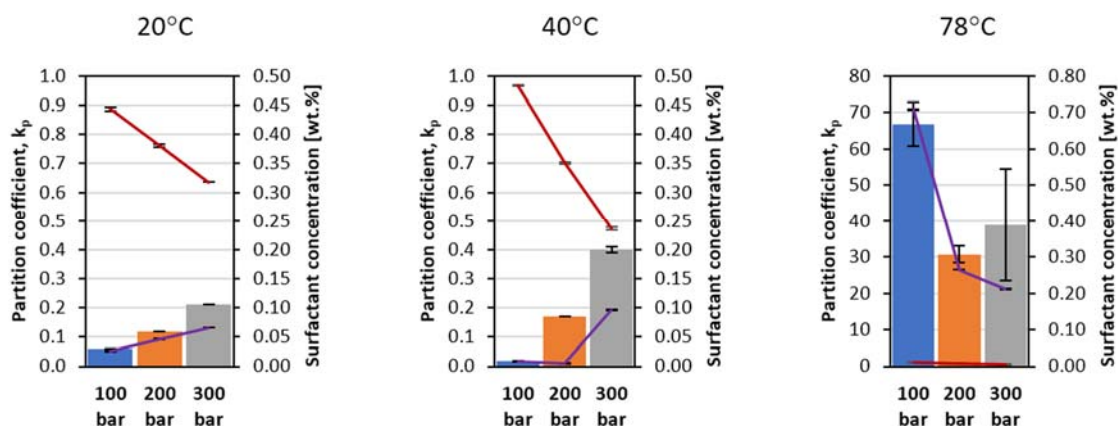
254 Igepal CA 720 showed similar surfactant distributions as Igepal CO 720. The same observations at
 255 100 bar and 40°C were made (Figure 10) as the preference for the CO₂ phase decreased compared to
 256 20°C. At 78°C, most of the surfactant was dissolved in the CO₂, 97.8 wt.% (100 bar), 98.2 wt.%
 257 (200 bar), and 98.9 wt.% (300 bar).



258

259 **Figure 10.** Surfactant distribution in SSW (blue) and in CO₂ (orange) for Igepal CA 720.

260 The partition coefficient followed the expected trend at 20°C and 40°C. It increased as both temperature
 261 and pressure increased with the exception of 100 bar (Figure 11). At 78°C, the partitioning coefficient
 262 decreased when the pressure was increased from 100 bar to 200 bar. The reduced partitioning
 263 coefficient, as well as the diminishing concentration in the CO₂ phase, is caused by the density effect
 264 explained previously.



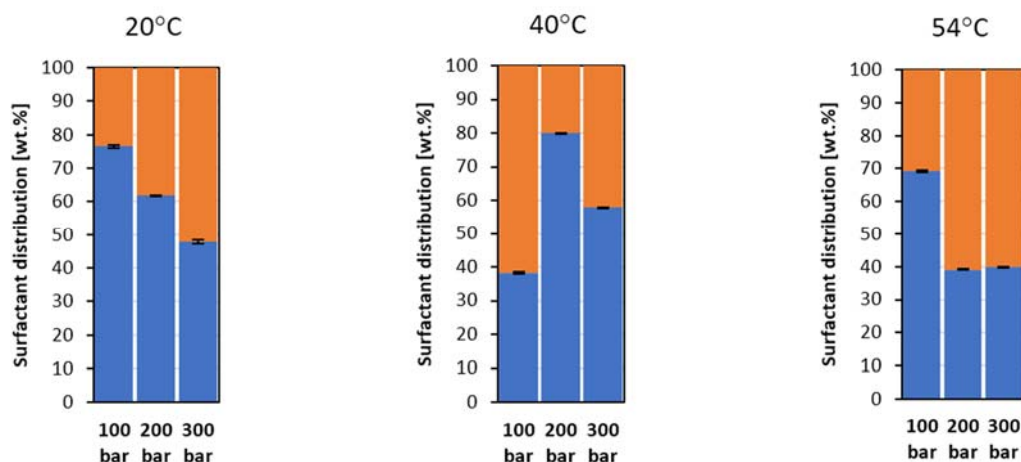
265

266 **Figure 11.** Partition coefficient for Igepal CA 720 (bars). In red line, residual surfactant concentration in SSW; in purple,
 267 surfactant concentration in CO₂.

268 *Tergitol NP 10*

269 Tergitol NP 10 did not follow any clear trend in its distribution between CO₂ and SSW (Figure 12). At
 270 20°C, the preference for the CO₂ phase increased as the pressure was increased. At 40°C, the CO₂
 271 distribution was higher 100 bar, lower for 200 bar, and higher for 300 bar, compared to 20°C. The lowest

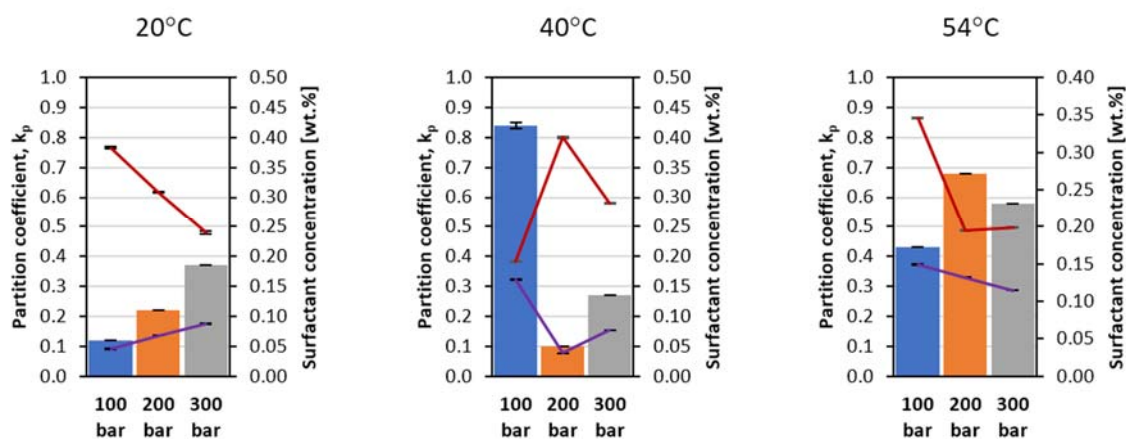
272 content in CO₂ was observed at 40°C and 200 bar where only 20 wt.% of the total surfactant was
 273 solubilized in the CO₂ phase. The largest content of surfactant in CO₂ was at 53.7°C both for 200 bar
 274 and 300 bar, where approximately 60 wt.% of the surfactant was in the CO₂ phase.



275

276 **Figure 12.** Surfactant distribution in SSW (blue) and in CO₂ (orange) for Tergitol NP 10.

277 At 20°C, the partition coefficient increased with pressure in accordance with the relative surfactant
 278 content. The largest coefficient was observed at 40°C and 100 bar (Figure 13). At 200 bar the coefficient
 279 decreased compared to 100 bar and increased when the pressure was increased to 300 bar. At 53.7°C,
 280 right below its cloud point, an opposite trend when compared to 40°C was observed. The coefficient
 281 increased from 100 to 200 bar and decreased again when the pressure was 300 bar.



282

283 **Figure 13.** Partition coefficient for Tergitol NP 10 (bars). In red line, residual surfactant concentration in SSW; in purple,
 284 surfactant concentration in CO₂.

285 4.3. Effect of concentration on partitioning

286 The effect of surfactant concentration on the partitioning was also studied for two surfactants, Tergitol
 287 TMN 10 and Brij L23. The results are depicted in Figure 14. The concentrations plotted are the residual
 288 concentration in SSW after equilibration at 40°C. The pressures used were 100, 200, and 300 bar.

289 For both surfactants, the increase of pressure promoted partitioning towards the CO₂ phase. However,
 290 as the concentration of surfactant in SSW increased, the partition coefficients decreased until plateau

291 values were reached (Figure 14). At 100 bar the partition coefficient for Tergitol TMN 10 exhibited an
 292 almost constant value (Figure 14.a) seemingly unaffected by concentration.

293 The partitioning coefficients were fitted to the exponential functions of the form:

294

$$k_p = A + Be^{-C \cdot Conc} \quad (2)$$

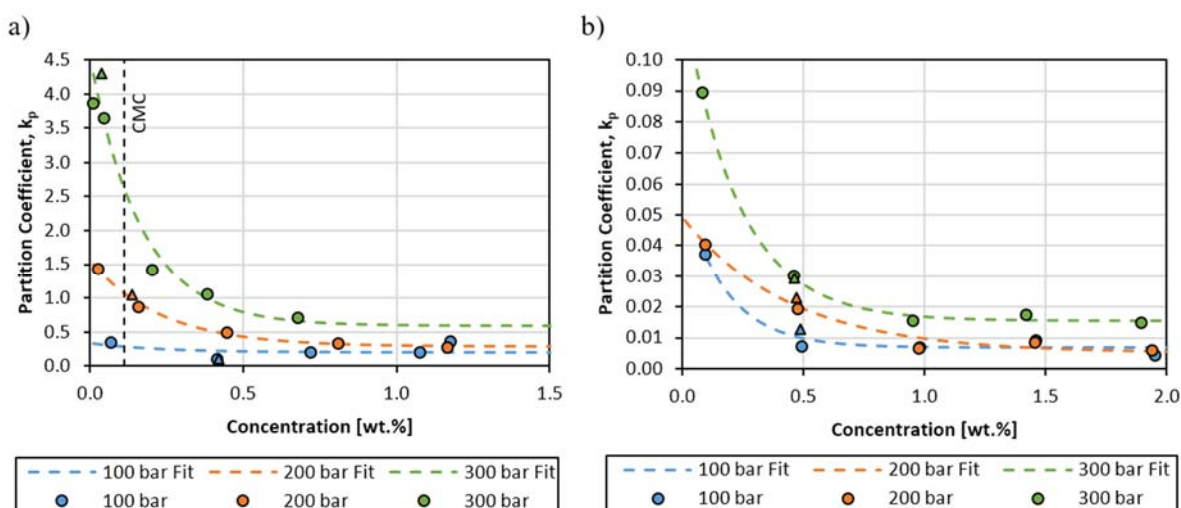
295 where k_p is the partition coefficient, $Conc$ is the surfactant concentration in SSW expressed in wt.%,
 296 and A , B , and C are empirical constants determined by the least-squares non-linear regression (Table 4).

297 **Table 4.** Equation 4 empirical constants determined for Tergitol TMN 10 and Brij L23.

Tergitol TMN 10				Brij L23			
	A	B	C		A	B	C
100 bar	0.1944	0.1390	4.3653	100 bar	0.0069	0.0518	5.7471
200 bar	0.2897	1.2740	4.3653	200 bar	0.0052	0.0439	2.2624
300 bar	0.5929	3.9281	5.9617	300 bar	0.0155	0.1054	4.3842

298

299 Figure 14 depicts the partition coefficient as a function of the surfactant concentration in SSW at
 300 equilibrium. The model gives a fair fit for all measurements.



301

302 **Figure 14.** Partition coefficient as a function of surfactant concentration at 40°C for a) Tergitol TMN 10 ($CMC_{aq} =$
 303 0.11 wt.%) and b) Brij L23 ($CMC_{aq} = 0.01$ wt.%). The data points marked with triangles correspond to a separate set of
 304 measurements.

305

306 5. Discussion

307 The surfactants selected for this research can be classified into two groups, alkyl ethoxylates and
 308 alkylphenol ethoxylates. Each group have similar ethoxylation numbers (except Brij L23) with carbon
 309 tails varying from linear to more branched structures. Nonetheless, a small variation on the CO_2 -philic
 310 moiety can have an important impact on the partition between aqueous and CO_2 phase. Also, some
 311 trends can be identified. One constant observation in all measurements (excepting Tergitol NP 10) was
 312 a decrease in the CO_2 solubility as temperature increased from 20°C to 40°C at 100 bar.

314 **5.1. Alkyl ethoxylates**

315 The partition in CO₂ was generally promoted as the degree of branching increased for the alkyl
316 ethoxylates. However, at temperatures up to 40°C, highly branched carbon chains could cause a
317 solubility decrease in CO₂. This could be explained by an increase in the "stiffness" of the CO₂-philic
318 moiety. Thus, as the solubility increases by the effect of increasing the methyl branching, it is
319 counteracted by a decrease of its conformational entropy, according to Flory and Huggins (Flory, 1953).
320 Above 40°C, Tergitol TMN 10 obtained a larger preference for the CO₂ phase than Tergitol 15-S-9.
321 However, the highest temperatures studied were not the same for both surfactants as the highest
322 temperature measured for each surfactant is limited by their cloud point.

323 Brij L23, the highly hydrophilic non-branched linear alkyl ethoxylate, the partitioning decreased as
324 temperature increased for 100 bar. This observation is in agreement with the research reported by Chen
325 *et al.* for similar surfactants at 117 bar for 24 and 40°C (Chen *et al.*, 2015). They explained it as a
326 lowered solvent strength of CO₂, which reflected a lowered tail solvation due to the decrease of density
327 and a weakened hydrogen bonding between the head groups due to the temperature increase. However,
328 the opposite trend was observed at pressures of 200 and 300 bar for increasing temperature. Here, as
329 CO₂ density decreased with increasing temperature, the surfactant solubility in CO₂ increased. Thus,
330 this observation cannot be explained by the lowered solvent strength and decreased tail solvation in CO₂.
331 A plausible explanation for the increased partitioning is that as solubility in the aqueous phase is
332 decreased with increasing temperature, surfactant partitions to the CO₂ phase and eventually starts
333 forming micelles. Thus, even if tail solvation in CO₂ is reduced, surfactant partitions to the CO₂ and
334 increases the micelle concentration.

335 A similar observation was made for Tergitol TMN 10 at 100 bar, where partition coefficient decreased
336 as temperature increased from 20 to 40°C. However, a further increase of temperature to 69°C, just
337 below systems cloud point, drastically increased the coefficient. Close to the cloud point, the weakened
338 hydrogen bonding between ethoxy-groups and water would favour surfactant migration towards CO₂.

339 **5.2. Alkylphenol ethoxylates**

340 Generally, increased pressure and temperature contributed to larger partition coefficients also for the
341 alkylphenol ethoxylates. At 100 bar, when the temperature was increased from 20°C to 40°C, the same
342 decrease in the partition coefficient observed with alkyl ethoxylates was also noticed.

343 Both Igepal CO 720 and Igepal CA 720 had similar solubilities into the CO₂, meaning that high
344 ramification of the CO₂-philic moiety did not have a major effect on their partition. Igepal CO 720 is a
345 linear alkylphenol ethoxylate with 9 carbons on its hydrophobic tail. Igepal CA 720 contains 8 carbons
346 but arranged in a highly ramified structure as it can be seen from Figure 1. It is also possible that the
347 aromatic ring in the CO₂-philic moiety influenced the partitioning. From the comparison between alkyl
348 ethoxylates and alkylphenol ethoxylates, it is observed that the presence of a benzene ring in the CO₂-
349 philic moiety has a slight detriment on its solubility and partitioning into CO₂ when temperatures were
350 not close to their respective cloud point.

351 For both surfactants, a decrease in the partition coefficient was observed at 100 bar when the temperature
352 was increased from 20 to 40°C. Further increase of temperature increased the coefficient, the same
353 observation noticed for the branched alkyl ethoxylates. The variations on the partitioning as pressure
354 and temperature are varied can only be explained by the balance between tail solvation in CO₂,
355 micellization in CO₂, and strength variation of the hydrogen bond interactions between water molecules
356 and hydrophilic headgroups.

357 Tergitol NP 10 can be considered as a medium branched alkylphenol ethoxylate. This surfactant did not
358 follow apparently any specific trend. When the temperature was increased from 20 to 40°C the partition
359 coefficients at 200 and 300 bar were reduced, while it increased for 100 bar. At 53°C, the effect was the
360 opposite; the partition coefficients increased at 200 and 300 bar but decreased at 100 bar (Figure 13).

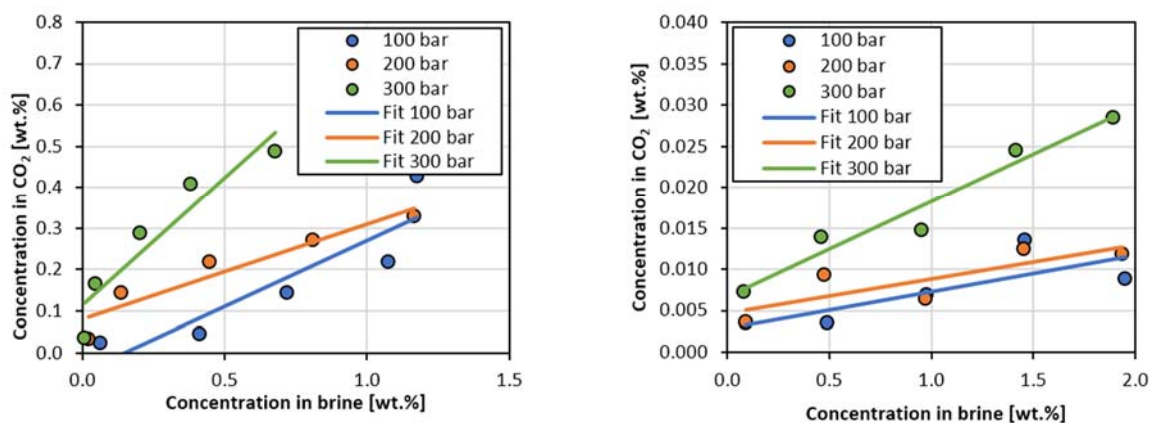
361 Compared to the other alkylphenol ethoxylates, Tergitol NP 10 had a low partition coefficient even
362 when the temperature was 2°C below its cloud point. For all studied conditions, the partition coefficient
363 never was above 1, obtaining the largest partition at 53.7°C and 200 bar ($k_p = 0.68$). Hence, Tergitol
364 NP 10 was the surfactant with the lowest observed CO₂ solubility in the study, the very hydrophilic
365 Brij L23 excluded. According to the conformational entropy approach, this surfactant should have
366 obtained the largest CO₂ solubility among the studied alkylphenol ethoxylates. However, this was the
367 case only for the measurements at 20°C and the measurement of 100 bar at 40°C, where the partition
368 coefficient was larger. Thus, the partitioning behaviour of this surfactant could not be properly
369 explained.

370 **5.3. Effect of concentration on partitioning**

371 In an ideal system, chemical components should have concentration-independent partition coefficients,
372 but for surfactants, there is a strong concentration dependence. Harusawa *et al.* studied the distribution
373 of octylphenol ethoxylates with different ethoxylation between isooctane and water system (Harusawa
374 *et al.*, 1980). For high ethoxylation numbers (EO 6 and 8) the surfactant concentration in the oil
375 increased up to the CMC and then remained constant for higher surfactant concentrations in the water.
376 For a low ethoxylation number (EO 4) the surfactant in the water phase remained constant after the
377 CMC was reached, whereas the concentration in the oil increased. This indicated that micelles were
378 formed in the oil phase. For an intermediate ethoxylation number (EO 5), the concentrations in both
379 phases remained constant after the CMC was reached and a separate surfactant-rich phase was formed.
380 Similar behaviour with constant concentrations in the oil phase (EO 6) or water phase (EO 8) after
381 reaching the CMC was observed in a system composed by water and cyclohexane using nonylphenol
382 ethoxylates (Harusawa *et al.*, 1980; Harusawa and Tanaka, 1981).

383 The systems studied in this work exhibited different behaviour. The continuous increase of the surfactant
384 concentration in the CO₂ phase beyond their respective CMCs, as it can be seen in Figure 15, has already
385 been observed and discussed (Balcan and Anghel, 2005). They noticed a slope change of the partition
386 isotherm at the CMC studying systems composed of n-hexane, water, and a commercial nonylphenol
387 ethoxylate with an average EO number of 10 as a surfactant. This behaviour resembles the one from
388 surfactant mixtures, where the partitioning increases beyond the CMC (Cowell *et al.*, 2000; Harusawa
389 *et al.*, 1982; Harusawa and Tanaka, 1981; Warr *et al.*, 1983). Commercial surfactants are molecules with
390 the same CO₂-philic moiety but with polydisperse EO numbers. Thus, they are surfactant mixtures with
391 dissimilar hydrophilic-lipophilic properties. After equilibration, the ethoxymer distribution was
392 measured in both phases and they observed that the aqueous phase contained larger mean EO numbers
393 than the n-hexane phase.

394 In the present study, the amount of surfactant in the CO₂ increased with an increased concentration in
395 the brine, as it can be observed in Figure 15. The CMCs of Tergitol TMN 10 and Brij L23 in water are
396 0.11 wt.% and 0.01 wt.%, respectively (given by the provider). These results are consistent with
397 previous observations (Balcan and Anghel, 2005) and with the theoretical partition model of
398 polydisperse ethoxylated surfactants.



399

400 **Figure 15.** Equilibrium surfactant concentrations in CO₂ and SSW for Tergitol TMN 10 (left) and Brij L23 (right).

401 6. Conclusions

402 The effects of branching, temperature, and pressure on the partitioning of non-ionic surfactants for SSW-
 403 CO₂ systems have been studied. Two main surfactant types were studied, alkyl and alkylphenol
 404 ethoxylates. Aside from Brij L23, all surfactants had a similar ethoxylation number. The effect of
 405 concentration on the partition coefficient was also studied for the surfactants Tergitol TMN 10 and Brij
 406 L23. For both surfactants, it was observed that the partition coefficient decreased with increasing
 407 surfactant concentration in the aqueous phase. The observations resemble the behaviour of surfactant
 408 mixtures as commercial surfactants have polydispersed EO numbers.

409 In general, alkyl ethoxylates showed a tendency of increased solubilization in CO₂ as both pressure and
 410 temperature increased. Branched alkyl ethoxylates (Tergitol 15-S-9 and Tergitol TMN 10) showed the
 411 largest solubilization in CO₂ at low temperature and pressure. At 100 bar and 20°C, 53 wt.% and
 412 62 wt.% of the surfactants solubilised in the CO₂, respectively. Brij L23, which is a linear alkyl
 413 ethoxylate with an ethoxylation number of 23, exhibited low solubilization up to 40°C. However, at
 414 80°C most of the surfactant solubilized in the CO₂ when the system was pressurized to 200 bar and
 415 300 bar. This observation was explained by the competitive effect between different mechanisms such
 416 as micellization in the CO₂, tail solvation in CO₂, and hydrogen bonding between ethoxylate groups and
 417 water molecules. Ramification increase of the hydrophobic tail is beneficial to increase CO₂ solubility
 418 to a certain degree for alkyl ethoxylates. Highly ramified tails might be detrimental possibly due to an
 419 increase of conformational entropy.

420 Alkylphenol ethoxylates showed lower solubilization than branched alkyl ethoxylates at 20°C and 40°C.
 421 However, high solubilisation in CO₂ was obtained both for Igepal CO 720 and Igepal CA 720 when the
 422 temperature was 2°C below their respective cloud points. The increase in solubilisation can possibly
 423 also be attributed to favourable interactions between ethoxylate groups and CO₂ as the hydrogen bonding
 424 with water molecules becomes weakened. Igepal CA 720 (branched alkylphenol moiety) obtained lower
 425 partition coefficients than Igepal CO 720 (linear alkylphenol moiety). This difference could be explained
 426 from the diminished conformational entropy that a more branched structure would have. No clear trend
 427 of tail ramification effect on CO₂ solubilization was identified for alkylphenol ethoxylates.

428

429

430

431

432 **Acknowledgement:** We acknowledge the Research Council of Norway for funding this work.
433 **Author Contributions:** The manuscript was written through the contributions of all authors. All authors have
434 given approval to the final version of the manuscript.
435 **Funding:** The present work was done as part of the project "Improved performance of CO₂ EOR and underground
436 storage by mobility control of CO₂" financed by the Research Council of Norway through the Climit Programme
437 (Grant number 267859).
438 **Conflicts of Interest:** The authors declare no conflicts of interest.
439

440 7. References

- 441 Adkins, S.S. *et al.*, 2010. Morphology and stability of CO₂-in-water foams with nonionic hydrocarbon
442 surfactants. *Langmuir*, 26(8): 5335-48.
- 443 Ashoori, E., van der Heijden, T. and Rossen, W.R., 2009. Fractional Flow Theory of Foam
444 Displacements With Oil (SPE-121579-MS), SPE International Symposium on Oilfield Chemistry.
445 Society of Petroleum Engineers, The Woodlands. Texas, pp. 17.
- 446 Balcan, M. and Anghel, D.F., 2005. The partition of ethoxylated non-ionic surfactants between two non-
447 miscible phases. *Colloid and Polymer Science*, 283(9): 982-986.
- 448 Bera, A., Kumar, T., Ojha, K. and Mandal, A., 2013. Adsorption of surfactants on sand surface in
449 enhanced oil recovery: Isotherms, kinetics and thermodynamic studies. *Applied Surface Science*, 284:
450 87-99.
- 451 Binks, B.P., 2002. Particles as surfactants—similarities and differences. *Current Opinion in Colloid &*
452 *Interface Science*, 7(1): 21-41.
- 453 Chen, Y. *et al.*, 2015. CO₂-in-Water Foam at Elevated Temperature and Salinity Stabilized with a
454 Nonionic Surfactant with a High Degree of Ethoxylation. *Industrial & Engineering Chemistry Research*,
455 54(16): 4252-4263.
- 456 Chen, Y. *et al.*, 2012. Ethoxylated Cationic Surfactants For CO₂ EOR In High Temperature, High
457 Salinity Reservoirs, SPE Improved Oil Recovery Symposium. Society of Petroleum Engineers, Tulsa,
458 Oklahoma, USA.
- 459 Cowell, M.A., Kibbey, T.C.G., Zimmerman, J.B. and Hayes, K.F., 2000. Partitioning of Ethoxylated
460 Nonionic Surfactants in Water/NAPL Systems: Effects of Surfactant and NAPL Properties.
461 *Environmental Science & Technology*, 34(8): 1583-1588.
- 462 Curbelo, F.D.S. *et al.*, 2007. Adsorption of nonionic surfactants in sandstones. *Colloids and Surfaces A:*
463 *Physicochemical and Engineering Aspects*, 293(1): 1-4.
- 464 Enick, R.M., Olsen, D., Ammer, J. and Schuller, W., 2012. Mobility and Conformance Control for CO₂
465 EOR via Thickeners, Foams, and Gels - A Literature Review, SPE Improved Oil Recovery Symposium.
466 Society of Petroleum Engineers, Tulsa, Oklahoma, USA.
- 467 Espinosa, D., Caldelas, F., Johnston, K., Bryant, S.L. and Huh, C., 2010. Nanoparticle-Stabilized
468 Supercritical CO₂ Foams for Potential Mobility Control Applications, SPE Improved Oil Recovery
469 Symposium. Society of Petroleum Engineers, Tulsa, Oklahoma, USA.
- 470 Flory, P.J., 1953. *Principles of Polymer Chemistry* Cornell University Press, Ithaca, New York.
- 471 Grimstad, A.-A., Bergmo, P., Nilsen, H.M. and Klemetsdal, Ø., 2018. CO₂ Storage with Mobility
472 Control, 14th International Conference on Greenhouse Gas Control Technologies, GHGT-14,
473 Melbourne, Australia.
- 474 Harusawa, F., Nakajima, H. and Tanaka, M., 1982. The Hydrophile-Lipophile Balance of Mixed
475 Nonionic Surfactants. *Journal of the Society of Cosmetic Chemists*, 33(3): 115-129.
- 476 Harusawa, F., Saito, T., Nakajima, H. and Fukushima, S., 1980. Partition isotherms of nonionic
477 surfactants in the water—cyclohexane system and the type of emulsion produced. *Journal of Colloid*
478 *and Interface Science*, 74(2): 435-440.
- 479 Harusawa, F. and Tanaka, M., 1981. Mixed micelle formation in two-phase systems. *The Journal of*
480 *Physical Chemistry*, 85(7): 882-885.
- 481 Hoefling, T.A., Enick, R.M. and Beckman, E.J., 1991. Microemulsions in near-critical and supercritical
482 carbon dioxide. *The Journal of Physical Chemistry*, 95(19): 7127-7129.
- 483 Johnston, K.P. and Rocha, S.R.P.d., 2009. Colloids in supercritical fluids over the last 20 years and
484 future directions. *The Journal of Supercritical Fluids*, 47(3): 523-530.
- 485 Le, V.Q., Nguyen, P. and Sanders, A.W., 2008. A Novel Foam Concept With CO₂ Dissolved
486 Surfactants, SPE/DOE Improved Oil Recovery Symposium. Society of Petroleum Engineers, Tulsa,
487 Oklahoma, USA.
- 488 Manlowe, D.J. and Radke, C.J., 1990. A Pore-Level Investigation of Foam/Oil Interactions in Porous
489 Media. SPE-27787-PA: 495-502.
- 490 McLendon, W.J. *et al.*, 2012. Assessment of CO₂-Soluble Surfactants for Mobility Reduction using
491 Mobility Measurements and CT Imag, SPE Improved Oil Recovery Symposium. Society of Petroleum
492 Engineers, Tulsa, Oklahoma, USA.

493 San, J., Wang, S., Yu, J., Lee, R. and Liu, N., 2016. Nanoparticle Stabilized CO₂ Foam: Effect of
494 Different Ions, SPE Improved Oil Recovery Conference. Society of Petroleum Engineers, Tulsa,
495 Oklahoma, USA.

496 Schramm, L.L. and Novosad, J.J., 1990. Micro-visualization of foam interactions with a crude oil.
497 Colloids and Surfaces, 46(1): 21-43.

498 Solbakken, J.S., Skauge, A. and Aarra, M.G., 2013. Supercritical CO₂ Foam - The Importance of CO₂
499 Density on Foams Performance, SPE Enhanced Oil Recovery. Society of Petroleum Engineers, Kuala
500 Lumpur.

501 Tsau, J.-S. and Grigg, R.B., 1997. Assessment of Foam Properties and Effectiveness in Mobility
502 Reduction for CO₂-Foam Floods, SPE International Symposium on Oilfield Chemistry. Society of
503 Petroleum Engineers, Houston, Texas, USA.

504 Vassenden, F., Holt, T., Moen, A. and Ghaderi, A., 2000. Foam Propagation in the Absence and
505 Presence of Oil, SPE/DOE Improved Oil Recovery Symposium. Society of Petroleum Engineers, Tulsa,
506 Oklahoma, USA.

507 Warr, G.G., Grieser, F. and Healy, T.W., 1983. Distribution of polydisperse nonionic surfactants
508 between oil and water. The Journal of Physical Chemistry, 87(22): 4520-4524.

509 Wasan, D.T., Koczko, K. and Nikolov, A.D., 1994. Mechanisms of Aqueous Foam Stability and
510 Antifoaming Action with and without Oil, Foams: Fundamentals and Applications in the Petroleum
511 Industry. Advances in Chemistry. American Chemical Society, pp. 47-114.

512 Xing, D. *et al.*, 2012. CO₂-Soluble, Nonionic, Water-Soluble Surfactants That Stabilize CO₂-in-Brine
513 Foams. SPE-169104-PA, 17(04): 1172-1185.

514 Xing, D. *et al.*, 2010. CO₂-Soluble Surfactants for Improved Mobility Control, SPE Improved Oil
515 Recovery Symposium. Society of Petroleum Engineers, Tulsa, Oklahoma, USA.

516 Yu, J., Liu, N., Li, L. and Lee, R., 2012. Generation of Nanoparticle-Stabilized Supercritical CO₂ Foams,
517 Carbon Management Technology Conference. Carbon Management Technology, Orlando, Florida,
518 USA.

519